

Int. J. Forest, Soil and Erosion, 2012 2 (3): 107-118

ISSN 2251-6387

© August 2012, GHB's Journals, IJFSE, Shabestar, Iran

*Research Paper***Incorporating The Effect Of Root Systems Of Forest Species Into Spatially Distributed Models Of Shallow Landslides**

Enrico Antonio Chiaradia, Gian Battista Bischetti, Chiara Vergani

Department of Agricultural Engineering, University of Milan, Italy

Received: 2011-12-21

Accepted: 2012-03-28

**Abstract:** In this paper, the stability model SINMAP was applied to a mountainous study area in order to include soil reinforcement exerted by root systems of forest species. Including root cohesion information in slope stability models, in fact, can lead to a better description of the shallow landsliding process and decrease the requirement for information on past landslides that is needed for model calibration. The study area is located in northern Italy (Lombardy Region) and was classified in seven forest regions with different species composition. A two-phase procedure was applied: first of all, a standard calibration approach led to a realistic and strongly-related set of parameters for each defined calibration region; secondly, multi-scenario criteria was applied in order to test different hypothetical sliding depths, with particular attention to root distribution profiles obtained from field surveys. A quantitative index (the Weighted Modified Success Rate) was used to test the results obtained by the stability model (both standard calibration and multiple scenario). The results showed that using forest categories to set up multiple calibration regions is very effective in standard calibration procedure. Moreover, potential sliding depth in each region was effectively identified at the depth where Root Area Ratio values fall below 0.1 % and the maximum available rooted soil cohesion is less than 5 kPa. In this way the multiple region calibration approach becomes feasible also when data on observed landslides are scarce and it can be used just to calibrate the hydrologic factor range.

**Keywords:** SINMAP; root cohesion; shallow landslide; forest; Lombardy

**This article should be referenced as follows:**

Chiaradia E A, Bischetti G B, Vergani C (2012). Incorporating The Effect Of Root Systems Of Forest Species Into Spatially Distributed Models Of Shallow Landslides, *International Journal of Forest, Soil and Erosion*, 2 (3): 107-118.

**Introduction**

Rainfall, earthquakes, storm waves, water-level changes or rapid stream erosion can induce instability phenomena on banks and hillslopes, causing hydrogeomorphological hazard phenomena such as mass movement of rock, debris or earth down slopes (Huabin et al., 2005).

Such phenomena can cause damage to people's lives and, in countries where sloping land has been developed, they are one of the main concerns that man has to face. In Italy alone, it has been estimated that about 21,000 hydrogeomorphological hazard events have occurred in recent years (www.apat.gov.it, 2003) and 44 billion Euros need to be spent (Luciani, 2008) to repair the resulting damage and control the associated risks (about 2.8% of Italian GDP in 2008; <http://dati.istat.it/>).

Due to the importance of hydrogeomorphic hazards, as a consequence, the scientific community has made great efforts to develop more and more sophisticated analysis of the processes driving instability phenomena, advocating a multi-disciplinary approach (geology, engineering, forestry, etc.). In such a context, many Authors stress the positive effect of vegetation to reinforce the soil, in shallow landslides in particular (Wu and Sidle, 1995; Collison and Anderson, 1996; Preston and Crozier, 1999; Dhakal and Sidle, 2003; Keim and Skaugset, 2003; Danjon et al., 2008; Wolter et al., 2010; Bathurst et al., 2010). In principle the action of plants has long been well known (e.g. Gilbert, 1877 cit. Marston, 2010; Bischetti et al., 2009), but it is still not fully understood, and it is rarely explicitly incorporated into landslide and bank stability modelling.

The interaction between vegetation and instability processes is actually very complex. Two main effects, however, are generally recognized to act by means of the presence of the root system (e.g. Greenway, 1987; Sidle and Ochiai, 2006): 1) hydrological effects influencing the water movement into the soil and 2) mechanical effects affecting the geotechnical properties of the soil.

One of the main hydrological effects is the change in soil hydraulic conductivity value. It is well known, in fact, that the presence of the root systems increases the number of macropores and then facilitates the underground flow, inducing a rapid transfer of water from top to deeper layers (Sidle et al., 2001; Huchida et al., 2001; Hencher, 2010; Nieber and Sidle, 2010). This effect is well described by an increase of conductivity in soils having a low matrix conductivity, which becomes two or three orders of magnitude greater where soil is rooted (Guan et al., 2010; Nieber and Sidle, 2010).

The consequence of such a process is of great relevance when the location of the potential saturation layer in a forested area is investigated. A great gradient between soil conductivities of sub-imposed soil layers, in fact, can generate conditions for potential instability (Nieber and Sidle, 2010).

A second well recognized significant hydrologic effect of vegetation is water suction, which decreases the soil water content (e.g. Coppin and Richards, 1990; Gray and Sotir, 1996). Suction can reach great values and sometimes plays the most relevant role in slope stabilization (Simon and Collison, 2002), but it dramatically reduces to zero or shows positive values during severe rainfall events (Rezaur et al., 2002; Simon and Collison, 2002; Sidle and Ochiai, 2006; Redding and Devito, 2010).

From the mechanical point of view, the presence of roots in the soil profile can induce a positive effect on slope stabilization by increasing the soil resistance. Such an effect is well recognized to be due to the mobilization of the tensile resistance of roots before their rupture, by means of root-soil friction (e.g. Gray and Sotir, 1996). In recent decades, many efforts have been made to quantify such action (Pollen and Simon, 2005; Simon et al., 2006; Pollen, 2007; Bischetti et al., 2009; Hales et al., 2009; Pollen-Bankhead and Simon, 2009; Mickovski et al., 2010; Loades et al., 2010; Schwarz et al., 2010a; Schwarz et al., 2010b; Thomas and Pollen-Bankhead, 2010). Nevertheless, the several models that have been proposed to produce landslide susceptibility maps do not explicitly include the results of the above studies (Montgomery et al., 1998; Borga et al., 2002; Casadei et al., 2003; Claessens et al., 2007; Talebi et al., 2008; Kuriakose et al., 2009).

The most common approach to shallow landslide modelling combines, in a Geographical Information Systems (GIS) framework, a simplified steady-state topography-based hydrological model with the infinite slope scheme (Dietrich et al., 1993; Montgomery et al., 1994; Wu and Sidle, 1995; Pack et al., 1998; Dietrich et al., 1998; Borga et al., 2002; van Beek, 2002; Simoni et al., 2008). The success of such an approach is due to the simplicity of the steady-state approach in managing the hydrologic condition of slopes and the power of GIS technology in managing spatially distributed data (particularly elevations). GIS, in fact, can increase the efficiency and the repeatability of the analysis (Huabin et al.,

2005) and permits us to capture, store and analyse geographical data. This also permits the implementation of different degrees of sophisticated conceptual models, with a relatively low cost in the effort necessary for the analysis.

Physically-based models are the typical approach adopted in landslide hazard mapping and, although several issues affect the modelling results, they have been proven to be very useful (e.g. Dietrich et al., 1998; Wu and Sidle, 1995; Borga et al., 2002; Montgomery et al., 1994; Duan et al., 2000; Pack et al., 1998, 2005; Marston, 2010).

The aim of the present paper is to incorporate information from studies on the root cohesion at different soil depths into space-distributed shallow landslide models.

Root cohesion values were evaluated via tensile resistance models applied by means of root density distributions with depth and root mechanical characteristics, obtained from surveyed data and laboratory tests. Slope stability was estimated by means of one of the most used space-distributed shallow landslide models, the Stability INdex MAPping, SINMAP, framework (Pack et al., 1998; 2005).

The performance of this combined approach was quantitatively measured comparing the model results with past landslides from inventory maps available for the investigated region.

## Material and Methods

### The study area

The study area is a sub-catchment of the River Serio (Val Seriana) located 100 km north-east of Milan (Figure 1). The basin covers about 657 km<sup>2</sup> and its elevation ranges from 270 m a.s.l. as minimum at the outlet, to a maximum of 3054 m a.s.l. The mean hillslope steepness is 30°.

The lithology is mainly limestone (over 40%), dolomite rock (24%), phyllite (16%), clastic sediments (8%), micaschist (5%) and other basic rock, partially or completely outcropped or covered by eluvial and glacial deposits. A true soil map for the whole area is not available, but local studies (AA.VV., 2008) and surveys indicate that in most cases the soil types are generally forest cambisol and regosol.

“Disturbed” forests dominate lower altitudes (from 274 to 1596 m a.s.l.) where the action of man has determined their characteristics; pioneer and invasive species represent a significant component and the most representative species is black locust (*Robinia pseudoacacia* L.). At the same elevation belt, sweet chestnut woods cover isolated areas, indicating a former presence of this species, which in Lombardy was intensively cultivated in the past. At higher elevations, forests are characterized by oak as associations, mainly *quercus-carpinetus* (from 300 to 1945 m a.s.l.) and beech, which colonizes the belt between mild temperate forests and conifers (from 438 to 1894 m a.s.l.). Conifer forests are dominated by Norway spruces (*Picea excelsa* L.) and larch (*Larix decidua* Mill.) with a presence of mountain pine (*Pinus mugo* Turra) at highest altitudes (418 to 2317 m a.s.l.).

### The stability model SINMAP

Stability INdex MAPping model, SINMAP (Pack et al., 1998), was used to determine potential failure areas according to a physical based approach. Among the different models we chose SINMAP because, according to the user guide, “SINMAP can be used for forest planning and management, forest engineering, ...” and it has been developed within a forest context (Pack et al., 2005) The model has been used in its free GIS software MapWindow plugin (Bischetti and Chiaradia, 2010).

SINMAP couples the infinite slope stability model and the assumption of hydrologic steady state to compute pore water pressure in the soil. In the infinite slope stability approach, the Factor of Safety (*FS*) is (Hammond, 1992):

$$FS = \frac{c_s + c_r + (\gamma_s D - \gamma_w D_w) \cos^2 \beta \tan \phi}{\gamma_s \cdot D \cdot \sin \beta \cdot \cos \beta} \quad (1)$$

where (Figure 2)  $c_s$  is the soil cohesion (kPa),  $c_r$  is the additional root cohesion (kPa),  $\gamma_s$  is the soil unit weight (kN/m<sup>3</sup>),  $\gamma_w$  is the water unit weight (kN/m<sup>3</sup>),  $D$  is the vertical soil depth (m),  $D_w$  is the vertical water depth (m),  $\beta$  is slope angle (°) and  $\phi$  is internal friction angle (°).

Hammond et al. (1992) evaluated the weight of each term in equation 1 and obtained that the most important factors to determine *FS* are (in top-down order): hillslope angle, depth of soil, frictional angle and cohesion. They also showed that cohesion is the factor that mainly influences *FS* in the case of thin and steep soils, while for other cases it is the friction angle. In the case of shallow landsliding, then, root cohesion is of crucial importance, particularly in saturated conditions and in cohesionless soils.

Introducing the variables:

$$C = \frac{c_s + c_r}{h \gamma_s} \quad (-), \quad r = \frac{\gamma_w}{\gamma_s} \quad (-), \quad w = \frac{D_w}{D} = \frac{h_w}{h} \quad (-) \quad (2)$$

where  $h = D \cos \beta$  is soil thickness.

Equation (1) can be rewritten as:

$$FS = \frac{C + \cos \beta (1 - wr) \tan \phi}{\sin \beta} \quad (3)$$

Adopting the TOPMODEL approach (Beven and Kirkby, 1979) in a modified version, the relative wetness ( $w$ ) is:

$$w = \min \left( \frac{Ra}{T \sin \beta}, 1 \right) \quad (4)$$

where  $T$  is the transmissivity (m<sup>2</sup>/h),  $R$  is the steady state recharge that is an estimation of the lateral discharge (m/h),  $a$  is the upslope drained area per unit contour length (m<sup>2</sup>/m).

$C$ ,  $R/T$  and  $\phi$  (noted as PHI in the SINMAP model) are the calibration parameters of SINMAP and they are introduced as minimum and maximum values, considered uniformly distributed. The user can decide to define a unique uniform region of application of the model with a constant set of calibration parameters (Single Calibration Region method) or identify several sub-areas in which to impose different calibration sets (Multiple Calibration Regions method).

According to the combination of the parameters, the values  $FS_{min}$  and  $FS_{max}$  can be obtained; on such a basis, to define the level of stability of the terrain, SINMAP introduces a Stability Index (*SI*).

The terrain where  $FS_{min} > 1$  is considered stable and  $SI = FS_{min}$ , where  $FS_{min} < 1$  there is the possibility of failure and  $SI$  is defined as the probability of  $FS$  to be greater than 1 ( $\text{Prob}(FS > 1)$ ); the terrain where  $FS_{max} < 1$ , that is  $\text{Prob}(FS > 1) = 0$ , is considered unconditionally unstable.

Arbitrarily, SINMAP classifies as *stable* the terrain where  $SI > 1.5$ , *moderately stable* where  $1.5 > SI > 1.25$  and *quasi stable* where  $1.25 > SI > 1.0$ . Where  $1.0 > SI > 0.5$  and  $0.5 > SI > 0$ , instabilities can occur with different probability; the limits  $SI = 0.5$  and  $SI = 0.0$  are called *lower* and *upper*

threshold respectively. Where  $SI < 0.0$ , Pack et al. (1998) argued that such areas, if not failed in reality, must be held in place by forces that are not accounted for in the model (e.g. outcrops or anthropic structures) and they called them *defended*.

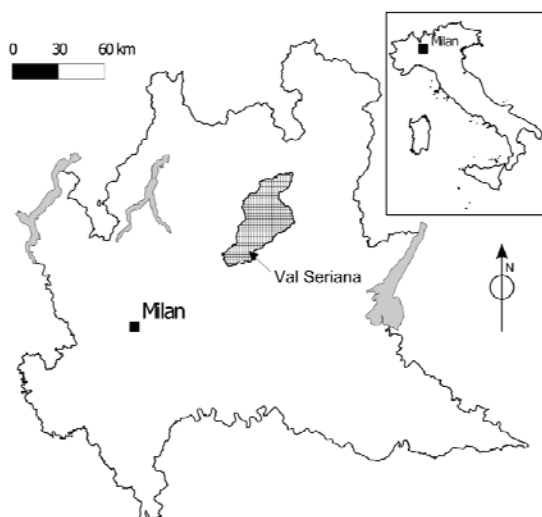


Figure 1. Study area.

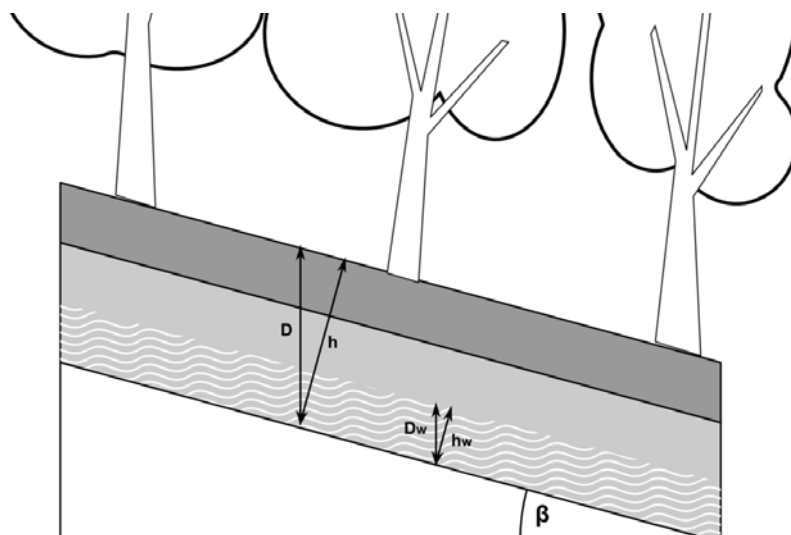


Figure 2. Infinite slope stability scheme (after Hammond et al., 2009)

More details about SINMAP are in the original papers of Pack et al. (1998; 2005) and papers dealing with SINMAP application (e.g. Meisina and Scarabelli, 2007; Terhorst and Kreja, 2009; Deb and El-Kadi, 2009; Bischetti and Chiaradia, 2010).

Calibration parameters must be adjusted based on the characteristics of the area and by comparing model results with historical landslides. Calibrating spatially distributed models, however, is a difficult task, especially on a qualitative basis and without an automatic optimization procedure. In the case of SINMAP, the common calibration procedure consists in an iterative manual adjustment of the parameters, based on a visual qualitative assessment of the output with respect to the observed landslides plotted in a Stability Analysis chart, SA Plot (Pack et al., 2005; Deb and El-Kadi, 2009; see Figure 5).

To limit subjectivity in the calibration procedure and to quantitatively evaluate model performance, in recent years several authors have proposed a success rate index, accounting for correctly modelled unstable areas (e.g. Montgomery and Dietrich, 1994; Borga et al., 2002; Duan and Grant, 2000).

According to Borga et al. (2002), two types of error can be identified in modelling slope instabilities: (1) a site is identified by the model as unstable, but no evidence of instability can be observed, (2) a site is predicted as stable, but instabilities have been observed. The first type of error indicates that the model tends to over-predict areas potentially subject to shallow landsliding, whereas the second indicates that the model does not adequately describe the processes that caused the instability process.

In principle, the first type of error may not be a true error because, especially in very steep areas, the predicted unstable condition could occur in the future. The second type of error, on the other hand, may have serious consequences when the considered model is applied to hazard mapping and it must be minimized.

The most common index adopted to evaluate the performance of stability models is the so-called Success Rate ( $SR$ ) (e.g. Montgomery and Dietrich, 1994; Borga et al., 2002; Duan and Grant, 2000), the ratio between the number of observed landslides that have actually occurred in predicted unstable areas ( $NU_R$ ) over the total number of observed landslides ( $NU_O$ ):

$$SR = NU_R / NU_O \quad (5)$$

When calibration is carried out in order to maximize  $SR$ , slope failure is over-predicted (e.g. Borga et al., 2002; Casadei et al., 2003; Huang et al., 2006) and more complex indexes were proposed (Huang et al., 2006; Rosso et al., 2006). In particular Huang et al., (2006) also considered, in addition to the correctly predicted landslides, the successfully predicted stable areas and developed a *Modified Success Rate*, which is an average between the success in predicting unstable and stable areas:

$$MSR = 0.5SR + 0.5 \frac{S_R}{S_O} \quad (6)$$

where, in a grid-based scheme of terrain,  $S_R$  are the successfully predicted stable cells and  $S_O$  is the total number of actual stable cells.

Due to the serious consequences of errors of the first type (Carrara et al., 1995), however, Bischetti and Chiaradia (2010) suggested that the two indexes should not have the same weight and introduced a Weighted Modified Success Rate ( $WMSR$ ) as a modification of Huang et al. (2006) and Rosso et al. (2006) indexes:

$$WMSR = \frac{2 \cdot U_R}{3 \cdot U_O} + \frac{S_R}{3 \cdot S_O} \quad (7)$$

where  $U_O$  is the number of observed unstable cells,  $S_O$  is the number of observed stable cells,  $U_R$  is the number of rightly simulated unstable cells and  $S_R$  is the number of rightly simulated stable cells.

The  $WMSR$  index should give a strong evaluation both of the calibration procedure and of the derived stability maps, overcoming the limits of subjective analysis.

#### Root cohesion estimation

To estimate the effect of roots on soil strength, we adopted the approach of Wu (1976) and Waldron (1977), W&W, which is the simplest and most used among those proposed in the literature. The W&W approach was coupled to the Fiber Bundle Model scheme, FBM (Pollen and Simon, 2005), to account for non-simultaneous breaking of the roots crossing the shear surface.

According to the W&W approach, root cohesion is a function of the mechanical resistance of each root element and its presence in the soil. Noting as  $T_r$  (MPa) the mechanical resistance of each element (tensile strength) and as  $a$  (mm<sup>2</sup>) the area of its section, the cohesion given by the presence of roots,  $c_r$  (kPa), is given by (Wu, 1976; Waldron, 1977):

$$c_r = k' \sum_{i=1}^N (T_r a_r)_i \quad (8)$$

where  $k'$  is a parameter that takes into account the inclination of roots in the soil.

Different Authors have assumed  $k'$  values ranging from 0.7 to 1.2 (Docker and Hubble, 2008); according to Bischetti et al. (2009) we considered a conservative value of one. Equation 8 returns the maximum value of root cohesion, whereas different studies reveal that the actual root reinforcement is less than the theoretical one, because roots exert their maximum resistance at different times (Riestedberg, 1994; Norris, 2005; Docker and Hubble, 2008). The sum of the roots area per reference soil area unit is commonly called the *Root Area Ratio* (RAR).

The FBM approach considers a bundle of parallel fibres loaded parallel to the fibres' direction, characterised by a statistically distributed strength. Fibres fail when the applied load exceeds a threshold value, and as consequence of failure, the load carried by the broken fibres is redistributed among the remaining intact fibres. This load redistribution consists of transferring stress from the broken to the unbroken fibres, inducing secondary failures that, in turn, induce tertiary ruptures, and so on. The failure avalanche terminates when the unbroken fibres are able to withstand the entire load or when the material collapses.

The FBM approach is affected by some critical issues (Bischetti et al., 2009), but at the moment it can be considered the most reliable in describing the process of non-simultaneous rupture of roots.

There are several ways to apply the FBM approach to the rooted soil condition (Thomas and Pollen-Bankhead, 2009); in our case we used a uniform and size-independent distribution of forces acting on the portion of rooted soil. The first assumption hypothesizes that the force distribution is not related to the position of the last-broken root; the second hypothesis assigns a constant value of stress force to each survived root, independently from its size.

In forests, generally, the plant density is high enough to cause root systems to overlap, making a dense root network which binds one plant to another. Generally, in fact, a continuous mattress of roots permeates the forest soil (Sakals and Sidle, 2004; Faser et al., 2005; Brisson and Reynolds, 1994; Casper et al., 2003; Schwarz et al., 2010b).

In such a context, when a layer of soil slips down, two shear surfaces have to be considered: a basal surface at depth  $z$  and a vertical (or lateral) surface between the soil surface and  $z$  (Schmidt et al., 2001; Roering et al., 2003). The whole reinforcement due to the presence of the root system, as a consequence, is due to the contribution of basal and lateral roots,  $C_{rb}$  and  $C_{rl}$  respectively. Bischetti et al. (2005) proposed to use eq. (8) for the basal cohesion estimation, and for the lateral cohesion the following equation:

$$c_{rl}(Z) = \sum_{j=1}^M \left[ c_{rbj} \frac{\Delta z_j}{Z} \right] \quad (9)$$

where  $M$  is the number of  $j$  layers of depth  $\Delta z_j$ ; that is, for constant depth classes  $\Delta z$ , the mean value of basal root cohesion along depth  $Z$ .

Data used in the present work derive from field work analyses executed in sites closed to the study area during a previous research project granted by Regione Lombardia-Agricultural Division.

RAR data were obtained for several dug profiles following the root-wall technique (Burke and Raynal 1994; Schmid and Kazda 2001, 2002; Vinceti et al., 1998; Xu et al., 1997) and applying image analysis (Vogt and Persson, 1991). For each image, roots were manually digitized, obtaining RAR values at depth increments of 10 cm (Bischetti et al., 2009).

Tensile strength of roots was obtained applying the testing procedure described in Bischetti et al. (2003, 2009). Roots were collected from each profile and either immediately tested or preserved in a 15% alcohol solution for some weeks without losses of mechanical properties (Meyer and Gottsche, 1971; Bischetti et al., 2005).

Finally, knowing the  $T_r$  and RAR values, root cohesion is determined by applying the model of W&W, coupled with FBM, according to Bischetti et al. (2009).

#### Including root cohesion into SINMAP

In a raster-based GIS framework, each cell of dimension  $l$  represents a portion of land where characteristics are homogeneous. In forested hillslopes, root density is commonly so high that resistance forces are over 10 times the proper soil cohesion (e.g. Abernethy and Rutherford, 2001; Schmidt et al., 2001; Bischetti et al., 2005; Bischetti et al., 2009; Hales et al., 2009), supporting the assumptions that the rooted layer of the whole cell works as a unique, homogeneous material and that it interacts with the adjacent cells.

Schmidt et al. (2001) introduced the effect of lateral roots cohesion,  $c_{rl}$ , in the infinite slope equilibrium formula (eq. 1), considering a lateral area,  $A_l$ , and a basal area,  $A_b$  where the basal root cohesion,  $C_{rb}$ , works:

$$FS = \frac{A_b c_s + A_b c_{rb} + A_l c_{rl} + A_b (\gamma_s D - \gamma_w D_w) \cos^2 \beta \tan \phi}{A_b \gamma_s \cdot D \cdot \sin \beta \cdot \cos \beta} \quad (10)$$

Rewriting eq. 10 in the form of SINMAP (eq. 3), the Factor of Safety becomes:

$$FS = \frac{A_b \left( c_s + c_{rb} + \frac{A_l}{A_b} c_{rl} \right) + A_b (\gamma_s D - \gamma_w D_w) \cos^2 \beta \tan \phi}{A_b \gamma_s \cdot D \cdot \sin \beta \cdot \cos \beta} \quad (11)$$

and the SINMAP cohesion factor,  $C$  (see eq. 2) assumes the form:

$$C = \frac{c_s + c_{rb} + \frac{A_l}{A_b} c_{rl}}{\gamma_s \cdot h} = \frac{c_s + c_{rb} + 3 \frac{D}{l} c_{rl}}{\gamma_s \cdot h} \quad (12)$$

where the influence of lateral roots for a pixel size block is estimated as  $A_l/A_b$  of lateral root cohesion value;  $A_l$  is calculated as three times the pixel dimension ( $l$ ) times the depth of the sliding surface in order to consider the effect of all the roots surrounding the sliding block and  $A_b$  is  $l^2$ .

In applying SINMAP, shear surface depth setting is a key point as expressed in eq. 2 and 12.

#### Workflow: model setup and evaluation of different sliding depth

Application of the stability model to the study area in order to investigate the effect of root systems on slope stability is described in the workflow of Figure 3.

First of all (step 1 in Figure 3), a Multiple Calibration Region of the model was carried out working on a set of calibration parameters (PHI,  $C$  and  $T/R$ ), different for each calibration region according to forest classes (see the study area section): 1) Evergreen coniferous forests, 2) Hydric forests, 3) Sweet chestnut woods, 4) European beech woods, 5) Anthropic "disturbed" forest, 6) Deciduous coniferous forests and 7) Thermophilous forests.

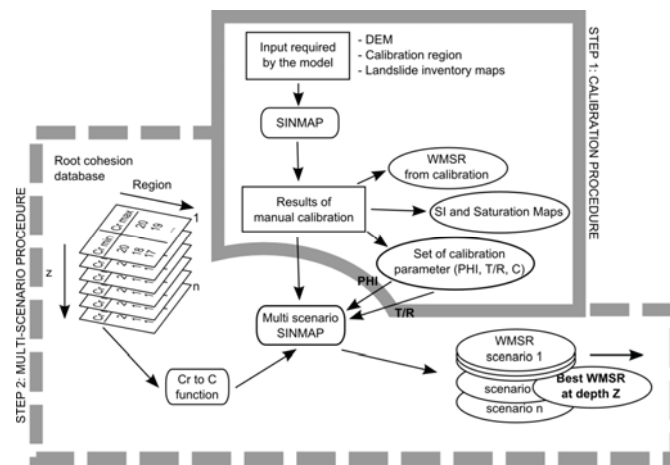


Figure 3. Workflow.

A regular grid size DEM with 20 m spacing (Territorial Information System of Regione Lombardia) was used for elevation. Past shallow landslides needed for model calibration and validation come from the landslide inventory of Regione Lombardia, IFFI (Ceriani and Fossati., 2006); a total of 101 events, dating from 1982, were taken into account and each event has been represented by a point marker.

Geotechnical properties have been assumed to be the same for all regions. Soil cohesion has been taken as negligible, soil friction angle (PHI) ranging between 20° and 30° (AA.VV., 2008) and soil unit density 20 kN/m<sup>3</sup> (Tofani et al., 2006).

The results of step 1 were: 1) the calibrated threshold values of  $T/R$  and  $C$  parameters (PHI values were taken as fixed), 2) the WMSR index for each calibration region and 3) stability index (SI) and saturation maps.

multi-scenario approach was implemented (step 2 in Figure 3) starting from the root profile analysis. Root Area Ratio ( $RAR$ ) and  $T_r$  were collected from field surveys and laboratory tests, and root cohesion values were estimated by the method previously illustrated. For each of the seven calibration regions the minimum and maximum value of  $c_r$  was calculated for each depth class (from 0.05 to 2.05 meters in depth) and SINMAP was run under 21 scenarios.

Minimum and maximum cohesion values at each depth were turned into  $C$  parameters, including the local cell-specific value of slope. The minimum  $C$  value was obtained considering only root basal cohesion while maximum values were estimated by eq. 9; in both cases, soil cohesion was considered negligible.

Multi-scenario tests resulted in a set of SI and saturation maps and a set of WMSR.

## Results

### RAR and root cohesion values

A synthesis of the mean root density and the associated cohesion is reported in Figure 4 where  $RAR$ , basal cohesion,  $Cr_{bas}$ , and total cohesion,  $Cr_{tot}$ , are plotted against depth.

$RAR$  distribution values follow, as is well-known, a decreasing trend with depth; in regions 1, 4, 5 and 6 the trend is very pronounced, whereas in regions 2, 3 and 7 it is less so. In the first case the maximum density near the surface arrives at values close to 1.5-2.0% (total  $RAR$ ), in the second the values are in the order of 0.5%. In all cases  $RAR$  approaches zero between 1.5 and 2.0 m, except for region 6 where roots are not present below 1 m.

Root cohesion (basal and total) decreases according to  $RAR$  distribution. As a consequence, maximum values of root cohesion are obviously located near the surface and decrease with depth. Root cohesion ranges between surface layers and 1 m: 15.11 to 1.78 kPa for evergreen coniferous, 12.13 to 1.35 kPa for hydric forests, 4.19 to 1.28 kPa for sweet chestnut woods, 21.76 to 2.43 kPa for European beech, 21.20 to 5.80 kPa for disturbed forests, 3.92 to 0.89 kPa for deciduous conifers, 8.60 to 1.57 kPa for thermophilous forests (Figure 4). Generally root cohesion approaches zero between 1.5 and 2.0 m, except for region 6 (deciduous conifer forest) where there is no root effect below 1 m.

Basal root cohesion reflects the trend of  $RAR$  distribution with two differences: 1) cohesion values are affected by a lower variability with respect to  $RAR$  along the descending trend, and 2) local increases in root cohesion are apparently not justified by corresponding local  $RAR$  values. Both of these effects are a consequence of the distribution of fine roots into soil layers. In the first case, in fact, total  $RAR$  values are mainly affected by the presence of thick roots that are not uniformly distributed in the soil profile. In the second case, there is an effect of the distribution of fine roots (which have greater  $T_r$  values), which are concentrated at 40-50 cm below the ground surface in deciduous conifer forests (region 6), whereas they are mainly at 95-135 cm and 75-115 cm in disturbed forests (region 5) and thermophilous forests (region 7) respectively.

distributions vary between different forest category: evergreen coniferous forests, beech woods and deciduous coniferous forests (regions 1, 4 and 6) show a clear difference between the high intensity rooted zone and low intensity-rooted zone; hydric forests, sweet chestnut woods and thermophilous forests (regions 2, 3 and 7) show a uniform descending trend; anthropic "disturbed" forest (region 5) shows a two-step shape with a higher rooted zone until 0.65 m in depth and a decreasing shape to null values after this limit.

Due to the relatively small influence of the lateral surface with respect to the basal area of a hypothetical sliding cell-size block, differences between basal and total cohesion values (the last calculated as summation between basal and a weighted portion of the lateral cohesion, see eq. 12) are generally very small.

### Standard SINMAP calibration

Charts of the relation between slope and contributing area for each calibration region (Pack et al., 1998; 2005) are reported in Figure 7: vertical lines represent stability index threshold and horizontal lines are saturation limits. The best fitting condition is obtained when most of landslide phenomena (black points in Figure 7) fall between the lower threshold ( $FS = 1.0$ ) and defended ( $FS = 0.0$ ) breaking lines. The best calibration condition happens when most of the landslides fall into the higher threshold class (e.g. Figure 7, region 7). In some cases, however, past landslides fall into stable classes (e.g. Figure 7, regions 1, 2, 4, 7) or defended areas (e.g. Figure 7, regions 1, 7); such cases should be considered as failures of the model settings or limits in the theory.

The parameter values giving the best fit are:  $T/R$  between 500 and 1000 for all calibration regions,  $C$  (minimum and maximum) varying considerably between different forest categories: 0.17 – 0.26 (region 1), 0.0 – 0.36 (region 2), 0.09 – 0.17 (region 3), 0.13 – 0.54 (region 4), 0.0 – 0.13 (region 5), 0.1 – 0.1 (region 6), 0.12 – 0.27 (region 7). Region 6 shows a unique value of  $C$ , i.e. all the variability is given by the PHI extremes.

The Modified Weighted Success Rates, MWSR, giving a measure of goodness of the calibration procedure, are: 63% (region 1), 43% (region 2), 58% (region 3), 63% (region 4), 74% (region 5), 70% (region 6), 63% (region 7). The average score is 62%.

Statistics from the calibration scenario, as reported in Table 1, show, according to the SI classes, how most of the land covered by forest is susceptible to manifest instability: 59% (region 1), 81% (region 2), 65% (region 3), 87% (region 4), 55% (region 5), 34% (region 6) and 70% (region 7). Only region 6 shows an instability region percentage less than 50%, but only because a consistent part of this region (56%) is characterized by defended areas (most of them rocks). Regions can be also ordered by their landslide density (Table 1): deciduous coniferous forests (region 6 - 0.09 landslides/km<sup>2</sup>), evergreen coniferous forests (region 1 - 0.12 landslides/km<sup>2</sup>), European beech woods (region 4 - 0.16 landslides/km<sup>2</sup>), thermophilous forests (region 7 - 0.23 landslides/km<sup>2</sup>), sweet chestnut woods (region 3 - 0.24 landslides/km<sup>2</sup>), anthropic "disturbed" forests (region 5 - 0.43 landslides/km<sup>2</sup>), and hydric forests (region 2 - 0.46 landslides/km<sup>2</sup>)

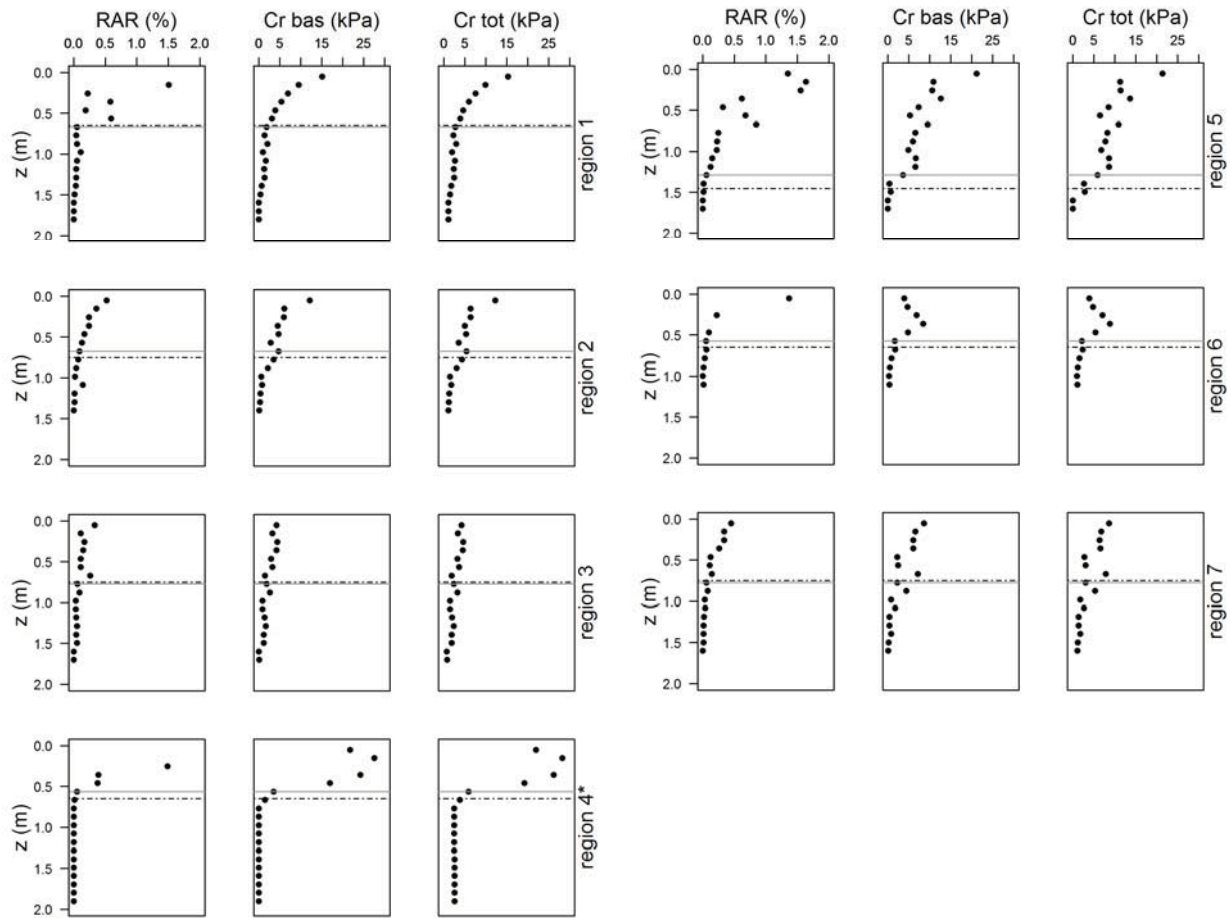


**Figure 4.** Average total RAR, basal and total cohesion for each depth class and calibration region; horizontal grey lines indicate significant changes in total RAR distribution (threshold value = 0.1%), black dot and dashed lines are the depth with the best WMSR for each calibration region (\* = total RAR values exceeded the limit of 2%).

### Multiple depth scenarios results

According to the workflow (Figure 3 - step 2), for each set of root cohesion values obtained by field and laboratory data (Figure 4), different shearing depths were considered in order to obtain different  $C$  values and to run SINMAP under different scenarios. The model performance (in terms of the resulting WMSR) for each depth and calibration region is presented in Figure 6 and Table 2.

WMSR values show a difference in model performance with depth. At small values of depth (i.e. the most superficial soil layer), WMSR is always low; the value of 33% obtained in any case means that only stable areas are correctly modelled by SINMAP, i.e. all the region (or most of it) falls into the stable class.

At deeper layers the model's performance varies; in some cases WMSR is higher (about 60%), in others it is the same and in others again it is lower (less than 20%).

Maximum WMSR values are generally comparable with WMSR obtained from the complete calibration procedure, except for regions 4 and 5, where the values differ for over 10% of the scores with respect to standard calibration.

The best performance (highest WMSR value) of the model for the different regions was obtained for depth values that were relatively constant, ranging between 55 and 75 cm, except for region 5 (anthropic "disturbed" forest) where the maximum is at 145 cm in depth.

In Table 3, total RAR, root cohesion and  $C$  factor thresholds are reported for each "best WMSR depth". Note that the SINMAP cohesion factor is calculated locally for each grid cell, while in Table 3, the  $C$  factors are determined assuming the average terrain slope calculated in each calibration region.

### Discussion

#### RAR distribution and root cohesion value

As shown in Figure 4, root density, expressed by RAR, follows a decreasing trend, as commonly reported in many studies (e.g. Bischetti et al., 2005; 2009; Macinnis-Ng et al., 2009; Abdi et al., 2010). Differences related to forest category (at least for the considered species) can be significant in terms of both maximum values and rate of decreasing with depth. Evergreen coniferous and deciduous forests, European beech woods and anthropic forests show the highest values of total RAR (maximum values exceed 2%), whereas hydric forests, sweet chestnut woods and thermophilous forests have maximum RAR values less than 1%.

In terms of depth, instead, all forest categories have roots at depth between 1.5 and 2.0 m, except deciduous coniferous forests where roots stop at about 1 m.

**Table 1.** Statistics from standard calibration procedure.

	Stable	Moderately Stable	Quasi-stable	Lower Threshold	Upper Threshold	Defended	Total
<b>Region 1</b>							
Area [km <sup>2</sup> ]	7.682	4.622	11.000	28.501	27.520	14.276	93.600
% of Region	8	5	12	30	29	15	100
#Landslides	1	0	0	5	4	1	11
% of slides	9	0	0	45	36	9	100
LS Density [# / km <sup>2</sup> ]	0.13	0.00	0.00	0.18	0.15	0.07	0.12
<b>Region 2</b>							
Area [km <sup>2</sup> ]	2.436	0.479	0.866	10.138	12.696	1.858	28.474
% of Region	9	2	3	36	45	7	100
#Landslides	5	0	1	3	4	0	13
% of slides	38	0	8	23	31	0	100
LS Density [# / km <sup>2</sup> ]	2.05	0.00	1.16	0.30	0.32	0.00	0.46
<b>Region 3</b>							
Area [km <sup>2</sup> ]	1.032	0.524	1.525	5.824	7.73	4.521	21.156
% of Region	5	2	7	28	37	21	100
#Landslides	1	0	0	2	2	0	5
% of slides	20	0	0	40	40	0	100
LS Density [# / km <sup>2</sup> ]	0.97	0.00	0.00	0.34	0.26	0.00	0.24
<b>Region 4</b>							
Area [km <sup>2</sup> ]	2.522	1.314	3.452	39.284	15.854	1.24	63.666
% of Region	4	2	5	62	25	2	100
#Landslides	0	0	1	7	2	0	10
% of slides	0	0	10	70	20	0	100
LS Density [# / km <sup>2</sup> ]	0.00	0.00	0.29	0.18	0.13	0.00	0.16
<b>Region 5</b>							
Area [km <sup>2</sup> ]	1.156	0.32	0.62	2.34	2.801	2.046	9.284
% of Region	12	3	7	25	30	22	100
#Landslides	0	0	0	3	1	0	4
% of slides	0	0	0	75	25	0	100
LS Density [# / km <sup>2</sup> ]	0.00	0.00	0.00	1.28	0.36	0.00	0.43
<b>Region 6</b>							
Area [km <sup>2</sup> ]	0.412	0.246	0.598	1.284	2.395	6.169	11.104
% of Region	4	2	5	12	22	56	100
#Landslides	0	0	0	1	0	0	1
% of slides	0	0	0	100	0	0	100
LS Density [# / km <sup>2</sup> ]	0.00	0.00	0.00	0.78	0.00	0.00	0.09
<b>Region 7</b>							
Area [km <sup>2</sup> ]	3.348	1.544	3.966	21.951	33.369	14.372	78.55
% of Region	4	2	5	28	42	18	100
#Landslides	0	1	0	6	10	1	18
% of slides	0	6	0	33	56	6	100
LS Density [# / km <sup>2</sup> ]	0.00	0.65	0.00	0.27	0.30	0.07	0.23

The data on root density distributions obtained in the present study are coherent with a qualitative description of soil profiles under forests. Schematically and with simplification, a soil profile under the forest canopy can be divided into different layers (Figure 5): a highly rooted zone (HRZ) commonly identified as the organic and A horizons, in our cases 30-50 cm depth, a low rooted zone (LRZ) generally identified as the B horizon, and a non-rooted soil layer (NRZ) identified as C horizon or bedrock. Many studies in forest ecology show that most of the root biomass is concentrated in the first layer and rapidly decreases after this depth (e.g. Macinnis-Ng et al., 2009; Finér et al., 2011). Roots, in fact, tend to grow near the surface because of the richness of nutrients, water and gases. Nonetheless, plant roots can run very long in depth (meters below soil surface) if the above factors are limited in shallower layers, but their density dramatically decreases with depth.

**Table 2.** MWSR for different depth of soil (Multi-scenario SINMAP application).

z (m)	Region						
	1	2	3	4	5	6	7
0.05	33	33	33	33	33	33	33
0.15	33	33	33	33	33	33	33
0.25	33	33	33	33	33	33	33
0.35	33	33	33	33	33	33	33
0.45	33	33	31	33	33	33	44
0.55	42	37	29	40	33	73	45
0.65	62	38	47	48	33	73	33
0.75	41	39	48	31	33	69	58
0.85	49	26	37	23	33	69	43
0.95	21	17	30	23	27	68	24
1.05	28	17	30	23	32	69	40
1.15	21	16	30	23	29	68	16
1.25	21	16	31	23	33	68	13
1.35	21	16	30	23	58	68	16
1.45	20	16	30	23	59	68	13
1.55	20	16	29	23	58	68	13
1.65	20	16	29	23	58	68	13
1.75	20	16	29	23	58	68	13
1.85	20	16	29	16	58	68	13
1.95	20	16	29	16	58	68	13
2.05	20	16	29	16	58	68	13
calibration	63	43	58	63	74	70	63

**Table 3.** Basal and total root cohesion ( $C_{rb}$  and  $C_{rt}$ ) and total RAR ( $RAR_t$ ) at each most potential sliding depth; mean region slope and  $C$  factor threshold for each calibration region.

ID	$Z_s$ (m)	$C_{rb}$ (kPa)	$C_{rt}$ (kPa)	$RAR_t$ (-)	slope (°)	$C$ min (-)	$C$ max (-)
1	0.65	1.87	2.72	0.05	31	0.17	0.25
2	0.75	3.51	4.34	0.07	30	0.27	0.34
3	0.75	1.91	2.39	0.06	28	0.15	0.18
4	0.65	1.45	3.83	0.01	35	0.14	0.37
5	1.45	0.65	2.83	0.01	24	0.03	0.11
6	0.65	1.8	2.40	0.06	33	0.17	0.22
7	0.75	2.31	3.09	0.06	34	0.19	0.25

RAR distribution is obviously affected by different local factors such as soil properties, species, aspect, morphology, position with respect to the main plants (Abdi et al., 2010), water availability, content of nutrients, etc. The interpretation of RAR distribution with respect to environmental factors is currently one of the topics under discussion in the scientific community, and it is beyond the objectives of the present paper. The illustrated scheme, however, is very useful in slope stability modelling, with particular reference to the potential sliding surface depth for the different forest categories.

#### Standard calibration

Standard calibration of SINMAP was based on  $T/R$  and  $C$  estimation by means of SA plots. Figure 7 shows a good agreement between observed landslides and model results: most of the events fall into the instability classes; outliers are probably due to errors in input data and limits of the physical model, as shown by Tarolli and Tarboton (2006).

The results show that most of the forested areas fall into the unstable condition. Such a result seems to reflect the site condition of forested slopes: high steepness and tendency to accumulate subsurface flow (i.e. convergent areas).

European beech woods (region 4), in particular, are the region which appears the most prone to manifest landslides although the density of actual landslides is in the same order of magnitude as other regions (Table 1). This can be explained by difficulties in mapping past landslides in densely covered areas that reduce the ability of remote recognition and field surveys (Brardinoni et al., 2003).

Hydric forests (region 2) and deciduous coniferous forests (region 6) are well interpreted by the model; the first has a considerable amount of unstable area coupled with the maximum value in landslide density, whereas the second has the smallest unstable area and the lowest landslide density (Table 1).

The range of the holistic hydrological parameter,  $T/R$ , which is the same for each calibration region, is lower than that proposed by the original Authors of the SINMAP model (Pack et al., 1998; 2005), but in agreement with other studies (e.g. Meisina and Scarabelli, 2007; Deb and El-Kadi, 2009; Bischetti and Chiaradia, 2010). The interpretation of the hydrological parameters is a difficult task since it summarizes different factors related to the translocation of water in soil and the influences of land use and morphology in the determination of landslide-

triggering rain events. According to the SINMAP Authors (Pack et al., 1998; 2005) the  $T/R$  parameters should be read as the planar upload slope necessary to obtain near-saturation conditions.

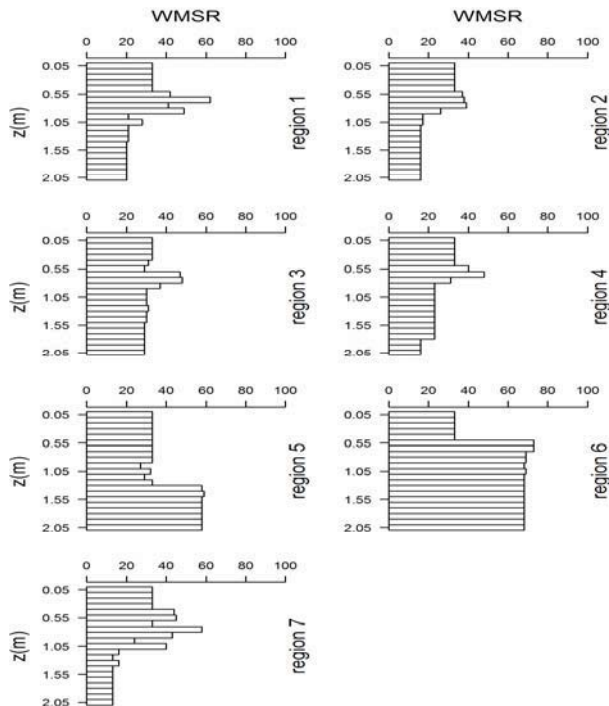


Figure 6. WMSR for each calibration region at different depths.

The  $C$  parameter assumes values similar to those reported in the bibliography (Pack et al., 1998; 2005; Meisina and Scarabelli, 2007; Bischetti and Chiaradia, 2010). Because the  $C$  factor includes both cohesion and the depth of the sliding surface, it is not possible to extract the actual contribution of the root system to slope stability without knowing the soil thickness.

#### Sliding depth determination

By adopting the multiple depth scenarios approach, the best root cohesion-sliding depth combination for each region has been obtained. This operation, which is a sort of back analysis of the past landslides in each region, was made possible by means of the use of the WMSR. The results seem to be robust in all calibration regions, except in regions 5 and 6 (anthropic “disturbed” forest and deciduous coniferous forest), where values of WMSR close to the best fitting condition extend to the maximum depth (2.05 meters), probably because of a lack of occurred landslides data.

Results show that the “best” sliding depth is always between 0.55 and 0.75 m, except in anthropic “disturbed” forest, where it is at 1.45 meters. Such findings agree with studies concerning sliding depth in forest areas (Schmidt et al., 2001; Roering et al., 2003) where sliding depths have been observed to range between 0.5 and 1 meter. In other cases, the sliding surface was hypothesized at depths up to 2 meters (e.g. Deb and El-Kadi, 2009) but study areas were located in deep volcanic soils.

In Figure 4, it can be observed that the “best” sliding depth is very close to the depth where total RAR values are less than 0.1%, except in region 5 where the difference in depth between the predicted sliding surface and the total RAR threshold is 0.2 m (see grey horizontal line in figure 4); RAR values for each sliding depth are: 0.05 (region 1), 0.07 (region 2), 0.06 (regions 3, 6 and 7), 0.01 (regions 4 and 5); the average value is 0.7 (Table 3).

At the same depths additional root cohesion values are always significant, basal root cohesion varies from 0.65 kPa (region 5) to 3.51 kPa (region 2), while total root cohesion varies from 2.40 kPa (region 6) to 4.34 (region 2), because of the influence of upper roots distribution.

In shallow landslides, it is commonly accepted that the critical depth occurs where a saturated layer rises and generally such a condition is a consequence of the combination of a permeable layer standing on another less permeable one. The presence of roots increases macropores and the richness of these last can induce great modification in the hydrological properties of soil, i.e. conductivity (Macinnis-Ng et al., 2009).

Under the above assumptions, the hypothetical sliding surface can be traced at soil depth corresponding to 0.1% of total RAR.

#### Conclusive remarks

The use of a spatially distributed model permits us to analyse the risk susceptibility for shallow landsliding. In this paper, the stability model SINMAP was applied to a mountainous area in order to include soil reinforcement exerted by root systems of forest species, drawing some advantages in respect to standard applications.

First of all, standard calibration of SINMAP can be carried out for both single and multiple regions calibration. In general, a multiple regions calibration approach should be preferred in order to account for spatial heterogeneity in hydrologic and geotechnical soil properties, but it requires more landslide data than the single region approach. In such a perspective, the present work shows that forest categories can be effective in identifying the different regions, where model parameters can be considered uniform.

The results obtained, moreover, according to the literature (e.g. Meisina and Scarabelli, 2007; Deb and El-Kadi, 2009; Bischetti and Chiaradia, 2010) show that SINMAP is more sensitive to the  $C$  than the  $T/R$  factor. The estimation of  $C$ , as a consequence, is a relevant issue in applying SINMAP and the use of information concerning root cohesion values with respect to depth has been proven to be very useful in order to estimate  $C$  without calibration, limiting the request of landslide data.

In each forest region, root cohesion values can be added to soil cohesion (if present), whereas the potential sliding surface can be derived from the analysis of  $RAR$  decay. The change in  $RAR$  values, in fact, seems to represent also a change in hydraulic conductivity which induces water accumulation at a depth where the transition from a densely rooted layer to a less densely rooted one occurs. The consequent saturation combined with a decrease in root cohesion makes such a depth the most probable for sliding.

In our case, for different forest categories, taking the sliding surface at the depth where  $RAR$  values drop below 0.1% led to the same model performance (quantitatively measured by MWSR) as that obtained by standard calibration.

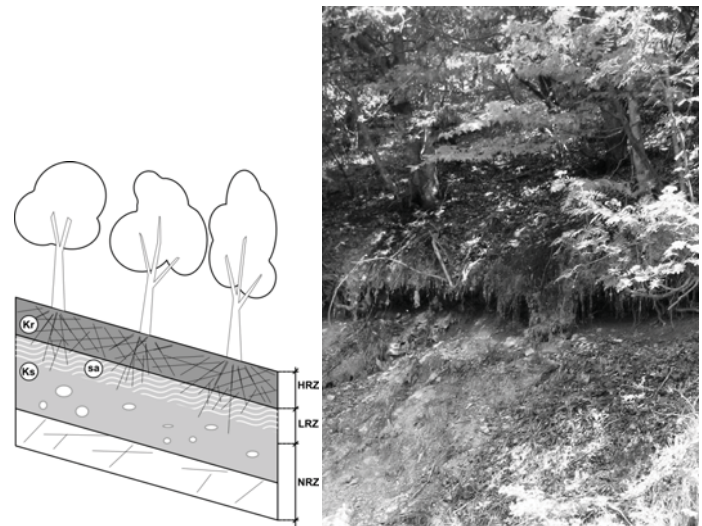


Figure 5. Rooted profile schema (left) and actual case with landslide in beech woods in Val Seriana (right).

The advantage of such an approach consists in the possibility of using the multiple region approach also when data on observed landslides are scarce and only one region can be considered. In such cases, in fact, data could be used to calibrate the  $T/R$  factor range for the whole area, whereas forest categories could be used to estimate the  $C$  factors for the different regions.

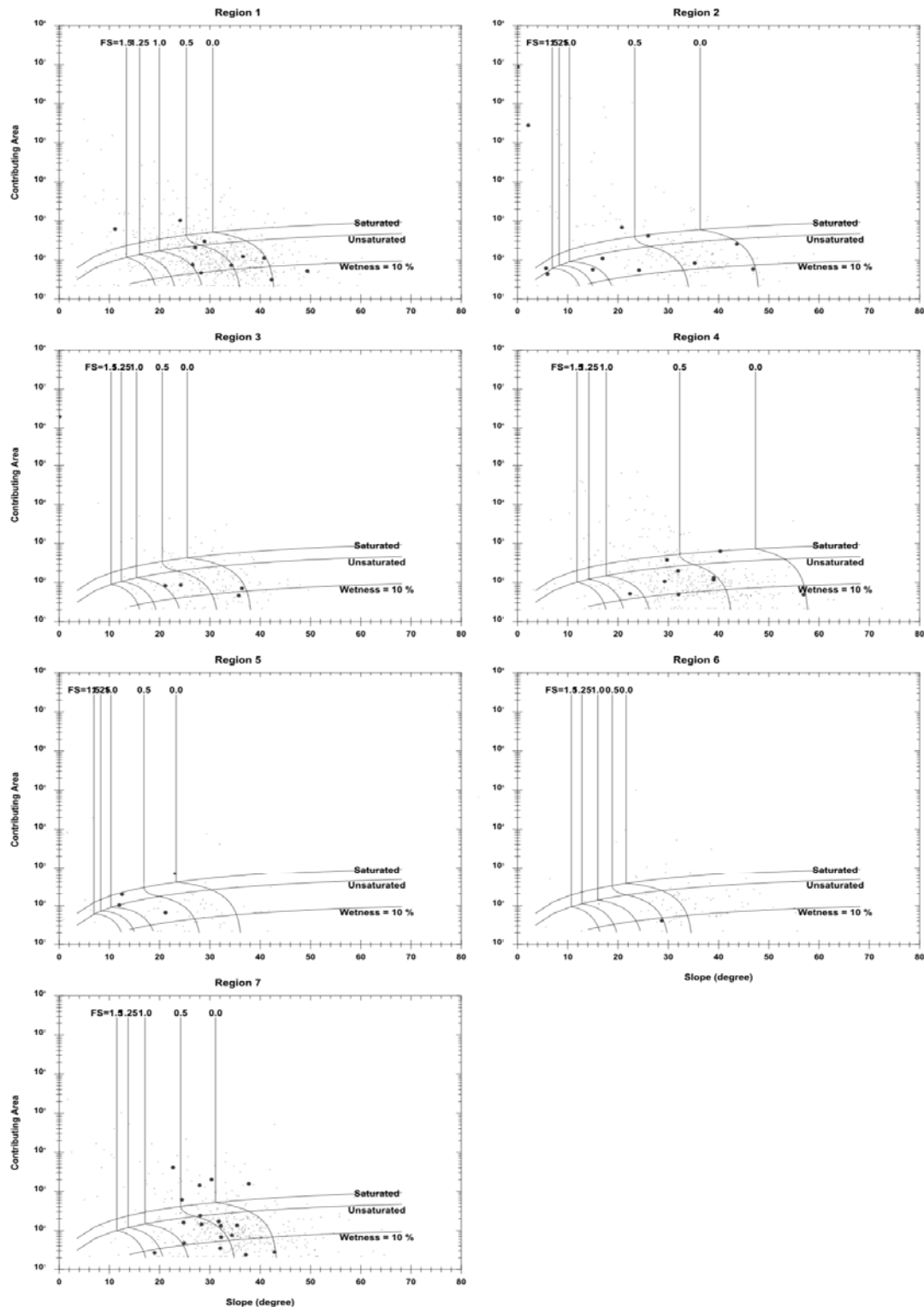


Figure 7. SA plots for each calibration region.

The findings of the present work on the potential sliding depth and root cohesion values at different depths can be used regardless of the stability model adopted.

The linkage between forest categories and sliding depth and root cohesion, finally, can be used by foresters and decision-makers in order to adopt management strategies for forest areas prone to shallow landsliding.

#### Acknowledgements

Data on root cohesion for the considered forest categories was obtained through the Project SISIFO granted by Regione Lombardia-DG Agricoltura. We thank Thomas Epis, Emanuele Morlotti, Eric Spelta and Marta Stropeni for field and laboratory work.

#### References

- AA.VV. (2008). Progetto strategico di potenziamento e collegamento dei demani sciabili dell'alta Val Seriana e della Val di Scalve. Analisi degli aspetti ambientali, progetto preliminare. (A design project to extend alpine skiing areas in the higher portion of the watershed; in Italian)
- Abdi E., Majnounian B., Genet M. & Rahimi H. (2010). Quantifying the effects of root reinforcement of Persian Ironwood (*Parrotia persica*) on slope stability; a case study: Hillslope of Hyrcanian forests, northern Iran. *Ecological Engineering* 36: 1409–1416. DOI: 10.1016/j.ecoleng.2010.06.020.

- Abernethy B. & Rutherford J.D. (2001). The distribution and strength of riparian tree roots in relation to riverbank reinforcement. *Hydrological Processes* 15: 63-79. DOI: 10.1002/hyp.152.
- Bathurst J.C., Bovolo C.I. & Cisneros F. (2010). Modeling the effect of forest cover on shallow landslides at the river basin scale. *Ecological Engineering* 36: 317-327. DOI:10.1016/j.ecoleng.2009.05.001.
- Beven K.J. & Kirkby M.J. (1979). A physically based variable contributing area model of basin hydrology. *Hydrological Sciences Bulletin* 24(1): 43-69.
- Bischetti G.B. & Chiaradia E.A. (2010). Calibration of distributed shallow landslides models in forested landscapes. *Journal of Agricultural Engineering* 41(3): 23-35. ISSN 1974-7071.
- Bischetti G.B., Bonfanti F. & Greppi M. (2003). Misura della resistenza alla trazione delle radici: apparato sperimentale e metodologia d'analisi. *Quaderni di Idronomia Montana* 241(1) (Measurement of the tensile strength of roots: experimental apparatus and test methodology; in Italian).
- Bischetti G.B., Chiaradia E.A., Epis T. & Morlotti M. (2009). Root cohesion of forest species in the Italian Alps. *Plant and Soil* 324: 71-89. DOI: 10.1007/s11104-009-9941-0.
- Bischetti G.B., Chiaradia E.A., Simonato T., Speziali B., Vitali B., Vullo P. & Zocco A. (2005). Root strength and root area ratio of forest species in Lombardy (Northern Italy). *Plant and Soil* 278: 11-22. DOI: 10.1007/978-1-4020-5593-5\_4.
- Borga M., Fontana G.D. & Cazorzi F. (2002). Analysis of topographic and climatic control on rainfall-triggered shallow landsliding using a quasi-dynamic wetness index. *Journal of Hydrology*. 268(1-4): 56-71. DOI:10.1016/S0022-1694(02)00118-X.
- Brardinoni F., Slaymaker H.O. & Hassan M.A. (2003). Landslide inventory in a rugged forested watershed: a comparison between air-photo and field survey data. *Geomorphology* 54: 179-196. DOI:10.1016/S0169-555X(02)00355-0.
- Brisson J. & Reynolds J.F. (1994). The effect of neighbours on root distribution in a Creosotebush (*Larrea tridentata*) population. *Ecology* 75: 1693-1702. DOI: 10.1111/j.1365-2745.2009.01500.x.
- Burke M.K. & Reynal D.J. (1994). Fine root growth phenology, production and turnover in a northern hardwood forest ecosystem. *Plant and Soil* 162: 135-146. DOI: 10.1007/BF01416099.
- Cammeraat E., van Beek R. & Kooijman A. (2005). Vegetation succession and its consequences for slope stability in SE Spain. *Plant and Soil* 278: 135-147. DOI: 10.1007/s11104-005-5893-1.
- Carrara A., Cardinali M., Guzzetti F. & Reichenbach P. (1995). GIS technology in mapping landslide hazard in Geographical Information Systems. In: *Assessing Natural Hazards*, Carrara A., Guzzetti F. (eds). Kluwer, 1995, The Netherlands, 135 - 175.
- Casadei M., Dietrich W.E. & Miller N.L. (2003). Testing a model for predicting the timing and location of shallow landslide initiation in soil-mantled landscapes. *Earth Surface Processes and Landforms* 28(9): 925-950. DOI: 10.1002/esp.470.
- Casper B.B., Schenk H.J. & Jackson R.B. (2003). Defining a plant's belowground zone of influence. *Ecology* 84: 2313-2321. DOI:10.1890/02-0287.
- Ceriani M. & Fossati D. (2006). *Inventario dei Fenomeni Franosi in Lombardia*. D.G. Protezione civile, Programma delle Ricerche Strategiche (Inventory of landslides in Lombardy Region; in Italian).
- Claessens L., Schoolt J.M. & Veldkamp A. (2007). Modelling the location of shallow landslides and their effects on landscape dynamics in large watersheds: An application for Northern New Zealand. *Geomorphology*. 87: 16-27. ISSN 0169-555X.
- Collison A.J.C. & Anderson M.G. (1996). Using a combined slope hydrology/stability model to identify suitable conditions for landslide prevention by vegetation in the humid tropics. *Earth Surface Processes And Landforms* 21(8): 737-747. DOI: 10.1002/(SICI).
- Coppin N.J. & Richards I.G. (1990). *Use of Vegetation in Civil Engineering*. Butterworths: London.
- Crosta G., Ambrosi C., Agliardi F., Frattini P. et al. (2004). Studio geologico, geotecnico, geomeccanico e di pericolosità del versante fronte lago comprendente i comuni di Colico, Dervio, Orino e Bellano. Regione Lombardia (Geological, geotechnical, geomechanical and danger study of the slope facing the lake covering the municipalities of Colico, Dervio, Orino and Bellano; in Italian).
- Danjon F., Barker D.H., Drexhage M. & Stokes A. (2008). Using three-dimensional plant root architecture in models of shallow-slope stability. *Annals of Botany*. 101: 1281-1293. DOI: 10.1093/aob/mcm199.
- Dhakal A.S. & Sidle R.C. (2003). Long-term modelling of landslides for different forest management practices. *Earth Surface Processes and Landforms*. 28: 853-868. DOI: 10.1002/esp.499.
- Deb S.K. & El-Kadi A.I. (2009). Susceptibility assessment of shallow landslides on Oahu, Hawaii, under extreme-rainfall events. *Geomorphology* 108: 219-233. DOI: 10.1016/j.geomorph.2009.01.009.
- Dietrich W.E. & Montgomery D.R. (1998). SHALSTAB: A digital terrain model for mapping shallow landslide potential. <http://calm.geo.berkeley.edu/geomorph/shalstab/theory.htm> (last visited: 1 April 2011).
- Dietrich W.E., Wilson C.J., Montgomery D.R. & McKean J. (1993). Analysis of erosion thresholds, channel networks and landscape morphology using a digital terrain model. *Journal of Geology* 101: 161-180.
- Docker B.B. & Hubble T.C.T. (2008). Quantifying root-reinforcement of river bank soils by four Australian tree species. *Geomorphology* 100 (3-4): 401-418. doi:10.1016/j.geomorph.2008.01.009.
- Duan J. & Grant G.E. (2000). Shallow landslide delineation for steep forest watersheds based on topographic attributes and probability analysis. In *Terrain Analysis: Principles and Applications*, Wilson JP, Gallant JC (eds.). Wiley & Sons: New York; 311-329.
- Faser E.C., Lieffers V.J. & Landhäusser S.M. (2005). Age, stand density, and tree size as factor in root and basal grafting of lodgepole pine. *Canadian Journal of Botany* 83: 983-988. DOI:10.1139/b05-048.
- Finer L., Ohashi M., Noguchi K. & Hirano Y. (2011). Factors causing variation in fine root biomass in forest ecosystems. *Forest Ecology and Management* 261: 265-277. DOI:10.1016/j.foreco.2010.10.016.
- Geertsema M. & Pojar J.J. (2007). Influence of landslides on biophysical diversity - A perspective from British Columbia. *Geomorphology* 89 (1-2): 55-69. DOI:10.1016/j.geomorph.2006.07.019.
- Gray D.H. & Sotir R.B. (1996). *Biotechnical soil bioengineering slope stabilization: a practical guide for erosion control*. Wiley: New York.
- Greenway D.T. (1987) *Vegetation and slope stability*. In *Slope Stability*. Eds. M G Anderson & K S Richards pp. 187-230. John Wiley, New York, USA.
- Guan H., Simunek J., Newman B.D. & Wilson J.L. (2010). Modelling investigation of water partitioning at a semiarid ponderosa pine hillslope. *Hydrological Processes* 24: 1095-1105. DOI: 10.1002/hyp.7571.
- Hales T.C., Ford C.R., Hwang T., Vose J.M. & Band L.E. (2009). Topographic and ecologic controls on root reinforcement. *Journal of Geophysical Research* 114: F03013. DOI: 10.1029/2008JF001168.
- Hammond C., Hall D., Miller S. & Swetik P. (1992). Level I, stability analysis (LISA) documentation for version 2.0. General Technical Report INT-285. USDA For Serv Intermt Res Stn.
- Hencher S.R. (2010). Preferential flow paths through soil and rock and their association with landslides. *Hydrological Processes* 24: 1610-1630. DOI: 10.1002/hyp.7721.
- Huabin W., Gangjun L., Weiya X. & Conghui W. (2005). GIS-based landslide hazard assessment: an overview. *Progress in Physical Geography* 29: 548-567. DOI: 10.1191/0309133305pp462ra.
- Huang J.C., Kao S.J., Hsu M.L. & Lin J.C. (2006). Stochastic procedure to extract and to integrate landslide susceptibility maps: an example of mountainous watershed in Taiwan. *Natural Hazards and Earth System Sciences* 6: 803-815. DOI:10.5194/nhess-6-803-2006.
- Hucida T., Kosugi K. & Mizuyama T. (2001). Effects of pipeflow on hydrological process and its relation to landslide: a review of pipeflow studies in forested headwater catchments. *Hydrological Processes* 15: 2151-2174. doi 10.1002/hyp.281.
- Keim R.F. & Skaugset A.E. (2003). Modelling effects of forest canopies on slope stability. *Hydrological Processes* 17: 1457-1467.
- Kuriakose S.L., van Beek L.P.H. & van Westen C.J. (2009). Parameterizing a physically based shallow landslide model in a data poor region. *Earth Surface Processes and Landforms* 34(6): 867-881. DOI: 10.1002/esp.1794.
- Loades K.W., Bengough A.G., Bransby M.F. & Hallett P.D. (2010). Planting density influence on fibrous root reinforcement of soils. *Ecological Engineering* 36: 276-284. DOI:10.1016/j.ecoleng.2009.02.005.
- Macinnis-Ng C.M.O., Fuentes S., O'Grady A.P., Palmer A.R., Taylor D., Whitley R.J., Yunusa I., Zeppel M.J.B. & Eamus D. (2009). Root biomass distribution and soil properties of an open woodland on a duplex soil. *Plant and Soil* 327(1-2): 377-388. DOI: 10.1007/s11104-009-0061-7.
- Marston R.A. (2010). Geomorphology and vegetation on hillslopes: interactions, dependencies and feedback loops. *Geomorphology* 116: 206-217. DOI:10.1016/j.geomorph.2009.09.028.

- Meisina C. & Scarabelli S. (2007). A comparative analysis of terrain stability models for predicting shallow landslides in colluvial soils. *Geomorphology* 87: 207–223. DOI:10.1016/j.geomorph.2006.03.039.
- Meyer F.H. & Göttsche D. (1971). Distribution of root tips and tender roots of beech. In *Ecological studies. Analysis and synthesis*, vol. 2, Ellenberg H (ed). Springer-Verlag: Berlin; 47–52.
- Mickovski S.B., Hallett P.D., Bransby M.F., Davies M.C.R., Sonnenberg R. & Bengough A.G. (2010). Mechanical reinforcement of soil by willow roots: Impacts of root properties and root failure mechanism. *Soil Science Society of America Journal* 73(4): 1276-1285. DOI:10.2136/sssaj2008.0172.
- Montgomery D.R. & Dietrich W.E. (1994). A physically based model for the topographic control on shallow landsliding. *Water Resources Research* 30: 1153–1171.
- Montgomery D.R., Sullivan K. & Greenberg H.M. (1998). Regional test of a model for shallow landsliding. *Hydrological Processes* 12(6): 943–955.
- Nieber J.L. & Sidle R.C. (2010). How do disconnected macropores in sloping soils facilitate preferential flow? *Hydrological Processes* 24(12): 1582-1594. DOI: 10.1002/hyp.7633.
- Norris J.E. (2005). Root reinforcement by hawthorn and oak roots on a highway cut-slope in Southern England. *Plant and Soil* 278(1-2): 43–53. DOI: 10.1007/s11104-005-1301-0.
- Pack R.T., Tarboton D.G., Goodwin C.N. & Prasad A. 2005. SINMAP 2 A stability Index approach to terrain stability hazard mapping. Version for ArcGIS 9.x and Higher. <http://hydrology.usu.edu/sinmap2/> (4 April 2011).
- Pack R.T., Tarboton D.G. & Goodwin C.N. (1998). The SINMAP approach to terrain stability mapping. In *Proceedings of 8th Congress of IAEG*, Vol. 2, Moore DP and Hungr O (eds.). Balkema: The Netherlands; 1157–1165.
- Pollen N. & Simon A. (2005). Estimating the mechanical effects of riparian vegetation on streambank stability using a fiber bundle model. *Water Resources Research* 41: W07025. DOI:10.1029/2004WR003801.
- Pollen N. (2007). Temporal and spatial variability in root reinforcement of streambanks: accounting for soil shear strength and moisture. *Catena* 69: 197–205. DOI:10.1016/j.catena.2006.05.004.
- Pollen-Bankhead N. & Simon A. (2009). Enhanced application of root-reinforcement algorithms for bank-stability modeling. *Earth Surface Processes And Landforms* 34: 471–480. DOI: 10.1002/esp.1690.
- Preston N.J. & Crozier M.J. (1999). Resistance to shallow landslide failure through root-derived cohesion in east coast hill country soils, North Island, New Zealand. *Earth Surface Processes and Landforms* 24: 665-675. DOI: 10.1002/(SICI)1096-9837(199908)24:8<665::AID-ESP980>3.0.CO;2-B.
- Redding T. & Devito K. (2010). Mechanisms and pathways of lateral flow on aspen-forested, Luvisolic soils, Western Boreal Plains, Alberta, Canada. *Hydrological Processes*. 24(21): 2995–3010. DOI:10.1002/hyp.7710.
- Rezaur R.B., Rahardjo H. & Leong E.C. (2002). Spatial and temporal variability of pore-water pressures in residual soil slopes in a tropical climate. *Earth Surface Processes and Landforms* 27: 317–338. DOI: 10.1002/esp.322.
- Riesterberg M.M. (1994). Anchoring of thin colluvium by roots of Sugar Maple and White Ash on hillslopes in Cincinnati. *United States Geological Survey Bulletin* 2059-E: 1–25. Roering J.J., Schmidt K.M., Stock J.D., Dietrich W.E. & Montgomery D.R. (2003). Shallow landsliding, root reinforcement and the spatial distribution of trees in the Oregon Coast Range. *Canadian Geotechnical Journal* 40: 237–253. DOI: 10.1139/T02-113.
- Rosso R., Rulli M.C. & Vannucchi G. (2006). A physically based model for the hydrologic control on shallow landsliding. *Water Resources Research* 42: W06410. DOI: 10.1029/2005WR004369.
- Sakals M.E. & Sidle R. (2004). A spatial and temporal model of root cohesion in forest soils. *Canadian Journal of Forest Research* 34: 950-958. DOI:10.1139/x03-268.
- Savage W.Z., Godt J.W. & Baum R.L. (2002). TRIGRS - A Fortran Program for Transient Rainfall Infiltration and Grid-Based Regional Slope-Stability Analysis. USGS <http://pubs.usgs.gov/of/2002/ofr-02-424/> (4 April 2011).
- Schmidt K.M., Roering J.J., Stock J.D., Dietrich W.E., Montgomery D.R. & Schaub T. (2001). The variability of root cohesion as an influence on shallow landslide susceptibility in the Oregon Coast Range. *Canadian Geotechnical Journal*. 38: 995–1024. DOI: 10.1139/cgj-38-5-995.
- Schmid I. & Kazda M. (2001). Vertical distribution and radial growth of coarse roots in pure and mixed stands of *Fagus sylvatica* and *Picea abies*. *Canadian Journal of Forest Research*. 31: 539–548. DOI: 10.1139/cjfr-31-3-539.
- Schmid I. & Kazda M. (2002). Root distribution of Norway spruce in monospecific and mixed stands on different soils. *Forest Ecology and Management*. 159: 37–47. DOI:10.1016/S0378-1127(01)00708-3.
- Schwarz M., Lehmann P. & Or D. (2010a). Quantifying lateral root reinforcement in steep slopes – from a bundle of roots to tree stands. *Earth Surface Processes and Landforms*. 35: 354–367. DOI: 10.1002/esp.1927.
- Schwarz M., Preti F., Giadrossich F., Lehmann P. & Or D. (2010b). Quantifying the role of vegetation in slope stability: a case study in Tuscany (Italy). *Ecological Engineering* 36: 285–291. DOI: 10.1016/j.ecoleng.2009.06.014.
- Sidle R.C., Noguchi S., Tsuboyama Y. & Laursen K. (2001). A conceptual model of preferential flow systems in forested hillslopes: evidence of self-organization. *Hydrological Processes* 15: 1675–1692. DOI: 10.1002/hyp.233.
- Sidle R.C. & Ochiai H. (2006). Landslides: processes, prediction and land use. *Water Resources Monograph* 18. American Geophysical Union: Washington DC.
- Simon A. & Collison A.J.C. (2002). Quantifying the mechanical and hydrologic effects of riparian vegetation on streambank stability. *Earth Surface Processes and Landforms*. 27(5): 527–546. DOI: 10.1002/esp.325.
- Simon A., Pollen N. & Langendoen E. (2006). Influence of two woody riparian species on critical conditions for streambank stability: Upper Truckee River, California. *Journal of the American Water Resources Association* 42(1): 99–113. DOI: 10.1111/j.1752-1688.2006.tb03826.x.
- Simoni S., Zanotti F., Bertoldi G. & Rigon R. (2008). Modelling the probability of occurrence of shallow landslides and channelized debris flows using GEOTOP-FS. *Hydrological Processes* 22(4): 532–545. DOI: 10.1002/hyp.6886.
- Talebi A., Troch P.A. & Uijlenhoet R. (2008). A steady-state analytical slope stability model for complex hillslopes. *Hydrological Processes* 22: 546–553. DOI: 10.1002/hyp.6881.
- Tarboton D.G. (1997). A new method for the determination of flow directions and contributing areas in grid digital elevation. *Models Water Resources Research* 33(2): 309-319.
- Tarolli P. & Tarboton D.G. (2006). A new method for determination of most likely landslide initiation points and the evaluation of digital terrain model scale in terrain stability mapping. *Hydrology and Earth System Sciences* 10: 663–677. DOI: 10.5194/hess-10-663-2006.
- Terhorst B. & Kreja R. (2009). Slope stability modelling with SINMAP in a settlement area of the Swabian Alb. *Landslides*. DOI 10.1007/s10346-009-0167-2
- Thomas R.E. & Pollen-Bankhead N. (2010). Modelling root-reinforcement with a fiber-bundle model and Monte Carlo simulation. *Ecological Engineering* 36: 47–61. DOI: 10.1016/j.ecoleng.2009.09.008.
- Tofani V., Dapporto S., Vannocci P. & Casaglini N. (2006). Infiltration, seepage and slope instability mechanisms during the 20-21 November 2000 rainstorm in Tuscany, central Italy. *Natural Hazards and Earth System Science* 6: 1025 – 1033.
- Van Beek H. (2002). Assessment of the influence of changes in land use and climate on landslide activity in a Mediterranean environment. PhD thesis, Utrecht University, <http://igitur-archive.library.uu.nl/dissertations/2003-0205-095231/inhoud.htm> (4 April 2011).
- Vinceti B., Paoletti E. & Wolf U. (1998). Analysis of soil, roots and mycorrhizae in a Norway spruce declining forest. *Chemosphere* 36: 937–942. DOI: 10.1016/S0045-6535(97)10151-5.
- Vogt K.A. & Persson H. (1991). Measuring growth and development of roots. *Techniques and approaches in forest tree ecophysiology*. CRC: Boca Raton.
- Waldron L.J. (1997). The shear resistance of root-permeated homogeneous and stratified soil *Journal of the Soil Science Society of America* 41: 843–849.
- Wolter A., Ward B., Millard T. (2010). Instability in eight sub-basins of the Chilliwack River Valley, British Columbia, Canada: a comparison of natural and logging-related landslides. *Geomorphology* 120(3-4): 123–132. DOI: 10.1016/j.geomorph.2010.03.008.
- Wu T.H. (1976). Investigation on landslides on Prince of Wales Island, Alaska. *Geotech Rpt No 5*, Dpt Civ Eng, Ohio State Univ, Columbus, US.
- Wu W. & Sidle R.C. (1995). A distributed slope stability model for steep forested basins. *Water Resources Research* 31: 2097–2110.
- Xu Y.J., Röhrig E. & Fölster H. (1997). Reaction of root systems of grand fir (*Abies grandis* Lindl.) and Norway spruce (*Picea abies* Karst.) to seasonal waterlogging. *Forest Ecology and Management* 93: 9–19. DOI: 10.1016/S0378-1127(96)03951-5